




Nectin-2 in ovarian cancer: How is it expressed and what might be its functional role?

Inga Bekes¹ | Sanja Löb² | Iris Holzheu¹ | Wolfgang Janni¹ | Lisa Baumann³ | Achim Wöckel² | Christine Wulff² 

¹Department of Obstetrics and Gynecology, University of Ulm, Ulm, Germany

²Department of Obstetrics and Gynecology, University of Würzburg, Würzburg, Germany

³Department of Pathology, University of Ulm, Ulm, Germany

Correspondence

Christine Wulff, Department of Obstetrics and Gynecology, University of Würzburg, Würzburg, Germany.
Email: webmaster@tine-wulff.de

Funding information

Deutsche Forschungsgemeinschaft, Grant/Award Number: DFG WU 319/3-2

Nectin-2 is an adhesion molecule that has been reported to play a role in tumor growth, metastasis and tumor angiogenesis. Herein, we investigated Nectin-2 in ovarian cancer patients and in cell culture. Tumor as well as peritoneal biopsies of 60 ovarian cancer patients and 22 controls were dual stained for Nectin-2 and CD31 using immunohistochemistry. Gene expression of Nectin-2 was quantified by real-time PCR and differences analyzed in relation to various tumor characteristics. In the serum of patients, vascular endothelial growth factor (VEGF) was quantified by ELISA. Effect of VEGF on Nectin-2 expression as well as permeability was investigated in HUVEC. In tumor biopsies, Nectin-2 protein was mainly localized in tumor cells, whereas in peritoneal biopsies, clear colocalization was found in the vasculature. T3 patients had a significantly higher percentage of positive lymph nodes and this correlated with survival. Nectin-2 was significantly upregulated in tumor biopsies in patients with lymph node metastasis and with residual tumor >1 cm after surgery. Nectin-2 expression was significantly suppressed in the peritoneal endothelium of patients associated with significantly increased VEGF serum levels. In cell culture, VEGF stimulation led to a significant downregulation of Nectin-2 which was reversed by VEGF-inhibition. In addition, Nectin-2 knockdown in endothelial cells was associated with significantly increased endothelial permeability. Nectin-2 expression in ovarian cancer may support tumor cell adhesion, leading to growth and lymph node metastasis. In addition, VEGF-induced Nectin-2 suppression in peritoneal endothelium may support an increase in vascular permeability leading to ascites production.

KEYWORDS

metastasis, Nectin-2, ovarian cancer, survival, VEGF

1 | INTRODUCTION

Ovarian cancer is a potential lethal gynecological malignancy which—as a result of a lack of early symptoms and suitable screening tests—is mostly diagnosed in an advanced stage of disease. Thus, ovarian cancer is associated with poor prognosis.¹ Although distant

metastasis is usually absent at the time of initial diagnosis, the main clinical characteristics of the disease are local tumor growth with early abdominal spread, consecutive development of ascites as a result of increased peritoneal permeability and early lymph node metastasis.²⁻⁴ Mechanisms responsible for these clinical observations are tumor cell proliferation, migration, adherence of tumor cells at

This is an open access article under the terms of the Creative Commons Attribution-NonCommercial License, which permits use, distribution and reproduction in any medium, provided the original work is properly cited and is not used for commercial purposes.

© 2019 The Authors. *Cancer Science* published by John Wiley & Sons Australia, Ltd on behalf of Japanese Cancer Association.

surfaces such as the peritoneum, thus forming new tumor bulk, and induction of angiogenesis.⁵ For these tissue remodeling processes, dynamic rearrangement of cell-cell junctions is essential. In this context, adhesion proteins of different cell junctions such as adherens junctions (AJ) and tight junctions (TJ) may play a distinct role.

The nectin-afadin system has recently been described as a novel modulator of AJ and TJ,⁶ acting as a cooperater system of AJ and TJ regulation.^{7,8} The nectins comprise a family of Ca²⁺-independent immunoglobulin-like cell adhesion molecules consisting of at least four members (nectin 1-4).⁹⁻¹⁴ Nectins are associated with the actin cytoskeleton through afadin, an F-actin-binding protein¹⁵⁻¹⁷ forming homophilic and heterophilic trans-dimers.⁷ Thereby, they function as cell-cell adhesion molecules and regulate the initial step of cell-cell junction formation of both AJ and TJ in epithelial and endothelial cells. Nectin-2—also termed cluster of differentiation 112 (CD112) and poliovirus receptor-related protein 2—is a transmembrane glycoprotein that interacts with various Nectin-like (Necl) molecules and different scaffold proteins regulating cellular functions such as proliferation cell movement, survival, cell adhesion and differentiation.¹⁸ These functions of Nectin-2 implicate its possible role in tumor cell survival and proliferation. So far, although only few investigations exist, the involvement of Nectin-2 in tumor pathogenesis has been described for different tumor entities, such as breast and ovarian cancer, but also for gallbladder, colorectal or pancreatic cancer.¹⁹⁻²¹ In some of these studies, high expression of Nectin-2 was associated with high malignancy, advanced tumor stage, poor differentiation, fast progression and poor outcome/prognosis.²⁰⁻²² At the same time, inhibition of Nectin-2 was followed by ceasing proliferation of tumor cells in cell culture. These studies indicate the high potential of Nectin-2 as a target for antibody therapeutics.

Despite its potential role in tumor cells, Nectin-2 has also been described as a surface marker of endothelial cells which—as an adhesion protein—might be involved in the regulation of endothelial migration, proliferation and permeability.¹⁸ Here, vascular endothelial growth factor (VEGF; and its interaction with adhesion molecules) is known to be the key regulator of angiogenesis and permeability regulation.²³ Our previous investigations have shown that increased peritoneal vascular permeability is due to VEGF-induced suppression of adhesion molecules in the peritoneal vasculature of ovarian cancer patients and is followed/associated with ascites production.²⁴

To further elucidate the potential role of Nectin-2 in ovarian cancer as well as its interaction and association with VEGF, we investigated the expression of Nectin-2 in human ovarian cancer tissue, which was collected over a period of 6 years from patients undergoing surgery compared to controls. Furthermore, we analyzed differences in expression concerning tumor biology, tumor stage, histological subtype, nodal metastasis, grading, estrogen/progesterone receptor expression and resection status after surgery as well as survival. As this cancer entity is frequently associated with increased vascular permeability of the peritoneum driven by tumor-derived VEGF, peritoneal biopsies of ovarian cancer patients were collected and Nectin-2 protein localization and gene expression investigated. Furthermore, serum levels of VEGF were measured in

tumor patients and controls to evaluate systemic VEGF interaction. Finally, the potential impact of VEGF on Nectin-2 expression in endothelial cells was tested *in vitro*.

2 | MATERIALS AND METHODS

2.1 | Patients

Tumor and peritoneal tissue as well as serum samples (for later VEGF analysis) were collected from patients undergoing laparotomy for ovarian cancer. Tumor samples were directly cut out of the main ovarian tumor (not from peritoneal metastasis). Peritoneal samples were collected from the paracolic gutter in regions not containing macroscopically visible metastasis. Tumor and peritoneal tissue samples were collected during surgery and placed in liquid nitrogen for further RNA isolation and in 3.5%-3.7% formaldehyde (Fischer, Saarbrücken, Germany) for immunohistochemistry. As controls, we used tissue samples of patients undergoing surgery for benign reasons such as uterine myoma or uterine prolapse. Serum samples of ovarian cancer patients and healthy patients were collected before surgery. Collection and use of human tissue were institutionally approved by the Ethics Committee of the University of Ulm and the patients had given their informed consent.

2.2 | Preparation of tissue for H&E staining and immunohistochemistry

Tumor and peritoneal tissue samples were fixed in 3.5%-3.7% formaldehyde (Fischer) for 24 hours and then incubated in 70% ethanol at room temperature overnight. Afterwards the tissue was dehydrated for each 2 × 45 minutes at 40°C in ascending concentrations of ethanol (95%-100%). Then tissue samples were placed in xylol and incubated for 2 × 45 minutes, followed by incubation in Paraplast Plus (Tissue Embedding Medium, Leica, Richmond, VA, USA) at 60°C for 2 × 60 minutes.

2.3 | Morphological characterization of ovarian cancer

Consecutive sections stained for H&E were used to classify the ovarian cancer and peritoneal tissue. Therefore, the embedded samples were serially sectioned, and tissue sections (3 μm) were placed onto SuperFrost Plus slides (VWR, Leuven, Belgium). Tissue sections were dewaxed in xylene, rehydrated in descending concentrations of ethanol, washed in distilled water and stained with hematoxylin (Mayer's hemalum solution; Merck, Darmstadt, Germany) for 3 minutes, followed by rinsing with hydrochloric acid 0.1% and by differentiation in flowing water for 5 minutes before staining with eosin (Eosin Y-solution 0.5% aqueous; Merck) and one drop glacial acetic acid/100 mL for 3 minutes, followed by washing in water. After dehydrating in ascending concentrations of ethanol and incubation with xylene, sections were mounted in Eukitt (Kindler, Freiburg, Germany).

Final histological tumor staging (TNM classification) was obtained from the report of the institutional pathologist and documented for each ovarian cancer patient for later analysis. Data on the intraoperative resection status (TR 0, no residual tumor; TR 1, residual tumor ≤ 1 cm; TR 2, residual tumor >1 cm) of each tumor patient were obtained from the operation report.

H&E-stained peritoneal sections from tumor patients were investigated for microscopic peritoneal metastasis. Only samples lacking microscopic metastasis were later used for Nectin-2 immunocytochemistry or RT-PCR analyses.

2.4 | Immunohistochemistry for specific cancer cell markers

Identification of ovarian cancer cells was carried out according to the WHO classification of tumors of female reproductive organs (2014).²⁵ For our analysis (of our shown example of endometrioid adenocarcinoma), antigen retrieval for immunohistochemistry was carried out as follows: anti-Vimentin staining: microwave oven; anti-estrogen receptor staining: Steamer (EDTA, pH 9); anti-Ki67 staining: pressure cooker; anti-CK7 staining: enzymatic pretreatment with pronase. Sections were incubated with the primary antibodies for 30 minutes in a Dako Autostainer (DAKO, Santa Clara, CA, USA). As primary antibodies, the following monoclonal mouse antihuman antibodies were used, diluted with antibody diluent (Zytomed Systems, Berlin, Germany): Vimentin (VIM 3B4, 1:300 dilution; Dako/Agilent [Dako, Santa Clara, CA, USA]), estrogen receptor (6F11, 1:50; Leica, Wetzlar, Germany), CK7 (OV-TL 12/30, 1:200; Dako/Agilent), and Ki67 (MIB-1, 1:200; Dako/Agilent). For visualization, a Dako REAL Detection System, Alkaline Phosphatase/RED, Rabbit/Mouse (DAKO, Santa Clara, CA, USA) was used, following the manufacturer's instructions. Slides were counterstained using hematoxylin.

2.5 | Immunohistochemistry dual staining of Nectin-2 and CD31

Immunofluorescence double-staining was carried out using a TSA-Kit (Perkin Elmer, Boston, MA, USA). Sections of paraffin-embedded cancer and peritoneal tissue were dewaxed and rehydrated using xylol and ethanol, respectively, and transferred to TN-buffer after a short wash in distilled water. Slides were incubated in Target Retrieval Solution pH 9 (1:10 dilution; Dako, Hamburg, Germany) at 95°C for 30 minutes in a water bath and cooled down at room temperature for another 20 minutes before being transferred to TN-buffer for 5 minutes.

Endogenous peroxidase was quenched for 30 minutes in 180 mL methanol + 20 mL hydrogen peroxide 30% (Fischar), and slides were again transferred to TN-buffer for 5 minutes. After preincubation with TNB for 30 minutes, the slides were incubated with mouse antihuman CD31 antibody (1:30 dilution; Dako) overnight at 4°C. The slides were then washed in TN-buffer with 0.1% Tween for 3 × 5 minutes, followed by incubation with biotinylated rabbit antimouse secondary antibody (dilution 1:750; Dako) for 45 minutes. Washing in TN-buffer

with 0.1% Tween for 15 minutes and incubation with Streptavidin-HRP Conjugate (NEL750; Perkin Elmer) for 30 minutes and fluorescein tyramide was done according to the instructions of the manufacturer. Incubation with the second primary antibody, the antibody rabbit antihuman Nectin-2/CD112 (NBP1-91211, 1:200 dilution; Novus Biologicals, Wiesbaden, Germany) overnight at 4°C was followed by washing, incubation with biotinylated goat antirabbit secondary antibody (1:500 dilution; Dako), Streptavidin-HRP Conjugate (NEL750; Perkin Elmer) and TMR tyramide as described above. Mounting was carried out with Roti-Mount FluorCare (Carl Roth, Karlsruhe, Germany). Pictures were taken with Keyence fluorescence microscope BZ-9000 (Keyence, Leinfelden, Germany) under 40× magnification.

2.6 | Image analyses

Quantitative analysis of immunostaining was carried out in randomly chosen high-power fields ($n = 5$ per section). The image analyzing system was set up to superimpose a grid (grid size 14 μm) over the selected fields. Number of points for CD31 (green fluorescence) or Nectin-2 (red fluorescence), respectively, was counted if staining reached a cross-point of the grid. Total number of CD31 crossing points was taken as 100% and the ratio of Nectin-2 staining then calculated. Values are expressed as mean + SEM for all analyzed fields per slide and specimen.

2.7 | Quantification of VEGF by ELISA

Analysis of our study focused on the most important pro-angiogenic factor VEGF-A (splice variant 165). In order to quantify the secreted amount of VEGF, a quantitative VEGF immunoassay was carried out according to the manufacturer's protocol (R&D Systems, Minneapolis, MN, USA). Briefly, 100 μL of sample and standard was added to 100 μL assay diluent. After 2 hours of incubation at room temperature, the samples were washed three times. Then, 200 μL VEGF conjugate was added for 2 hours before the samples were washed again. After incubation with 200 μL substrate solution for 25 minutes protected from light, 50 μL stop solution was added and the optical density was measured at 450 nm (ELISA reader, Sunrise; Tecan, Männedorf, Switzerland).

2.8 | Endothelial cell isolation of HUVEC

Collection of human primary cells was institutionally approved after favorable ethical review. Human umbilical cords were rinsed with water and disinfected with isoseptol. Under sterile conditions the ends of the cords were cut and, into each end, a flexible tube was inserted and fixed with a cable tie. The umbilical veins were rinsed with PBS (1 × PBS). One end was clamped and, from the other end, the vein was filled with Type I-A collagenase 1 mg/mL (100 mg; Sigma, Saint Louis, MO, USA) to detach the endothelial cells. Subsequently, the second end was clamped and the cords were incubated in 1 × PBS in a water bath at 37°C for 15 minutes. HUVEC were collected and mixed 1:1 with endothelial cell growth medium

(C-22010; PromoCell, Heidelberg, Germany) + 10% FCS with 1% penicillin/streptomycin (Gibco Life Technologies, Carlsbad, CA, USA). After centrifugation for 5 minutes at 290 g, the supernatant was discarded and the pellet was resuspended in culture medium. HUVEC were seeded in Primaria tissue flasks (25 cm²) (BD Falcon, Bedford, MA, USA) and incubated at 37°C in 5% CO₂.

2.9 | Stimulation and RNA isolation of HUVEC

Endothelial cells were stimulated in six-well plates for 48 hours with 500 ng/mL VEGF alone, 5000 ng/mL Flt-1/Fc alone and 500 ng/mL VEGF + 5000 ng/mL Flt-1/Fc (VEGF, Sigma; VEGF Receptor-1 [Flt-1]/Fc Chimera; Sigma). Total RNA from HUVEC was extracted from cells with the RNeasy Mini Kit (Qiagen, Hilden, Germany) according to the manufacturer's instructions. RNA was quantified by absorbance at 260 nm, and total RNA (1 µg) was reverse transcribed into cDNA using a cDNA High Capacity Reverse Transcription Kit (Applied Biosystems, Foster City, CA, USA) in accordance with the manufacturer's protocol. RT-PCR was carried out as described below.

2.10 | Preparation of tissue for RNA isolation

Pulverized tumor and peritoneal tissue (50-100 mg) was mixed with 1 mL peqGOLD TriFast reagent (Peqlab, Erlangen, Germany), incubated at room temperature for 5 minutes and mixed with 200 µL chloroform. After 3-5 minutes incubation at room temperature and centrifugation, the aqueous phase was mixed with 500 µL isopropanol and incubated for 5-15 minutes at 4°C. After centrifugation, the pellet was washed twice with 1 mL of 75% ethanol in diethylpyrocarbonate (DEPC)-H₂O and centrifuged for another 10 minutes at 4°C. Then the pellet was dispensed in RNA-free H₂O for 10 minutes at 55°C. RNA was measured on a spectrophotometer at 260 nm (NanoDrop 2000; Peqlab) and stored at -80°C.

2.11 | Human ovarian surface epithelial cells and reverse transcription

As control for our tumor samples, Human Ovarian Surface Epithelial Cell total RNA (HOSEpiC #7315; 3H Biomedical, Uppsala, Sweden) already prepared by manufacturer from early passage human ovarian surface epithelial (OSE) cells using the Qiagen AllPrep DNA/RNA Mini kit) was used and reverse transcribed into cDNA.

Total RNA (1.0 µg) was reverse transcribed into cDNA using the High Capacity cDNA Reverse Transcription Kit (Applied Biosystems, Foster City, CA, USA) according to the manufacturer's instructions.

2.12 | Real-time-PCR

For quantification of Nectin-2 expression, TaqMan Gene Expression Assays for Nectin-2 (Hs01071562) was used according to the manufacturer's instructions using TaqMan Universal PCR Master Mix (Applied Biosystems/Life Technologies, Darmstadt, Germany). Amplification and detection of specific products was carried

out with ViiA 7 Real-Time PCR System (Applied Biosystems/Life Technologies). As internal controls, two housekeeping genes HSP90AB1 (Hs01546471_g1) and β2-microglobulin (Human B2M; Applied Biosystems) were used and the quantity of cDNA was normalized to the quantity of both cDNAs in each sample. Calculation of relative gene expression was done using the comparative 2^{-ΔΔCT} method.²⁶ This method made it possible to determine the fold change in gene expression compared to control and create linear data from exponential values.

2.13 | Small interfering RNA knockdown of Nectin-2

For our knockdown experiments 1 day before transfection, 8 × 10⁵ cells were seeded into Primaria cell culture flasks T25 (BD Falcon) and cultured under normal growth conditions (37°C; 5% CO₂). Cells were then washed with PBS, and 2 mL growth medium was added. The transfection reagent contained (per T25 flask) 400 µL culture medium without serum, 6 µL negative control siRNA (20 nmol, 1027281; Qiagen) or Nectin-2 (mixture of nectin 2_5 siRNA Qiagen SI04950442, nectin 2_6 siRNA Qiagen SI04950449, and nectin 2_7 siRNA Qiagen SI04950456, each 5 nmol) and 12 µL HiPerFect transfection reagent (Qiagen). The transfection medium was incubated at least for 5 minutes to allow for the formation of transfection complexes before it was added to 2 mL of the endothelial cell growth medium. After 48 hours, transfection was repeated as described. After 72 hours, RNA was isolated for confirmation of a successful knockdown. The permeability assays were carried out for the same times.

2.14 | Permeability assay (in knockdown experiments)

To test the permeability of endothelial cells for macromolecules, HUVEC were seeded into an insert to allow the flow of dye through the membrane. HUVEC were seeded on micropore inserts (pore size 0.4 µm) at a density of 3 × 10⁵ cells per insert and cultured overnight. The next day, BSA was labeled with Trypan blue (66.7 mg Trypan blue to 1.6 g BSA in 40 mL PBS), mixed with culture medium 1:1, and added to the insert, whereas unlabeled albumin was added to the lower compartment. Samples of the wells were taken after 10 and 30 minutes and measured for color intensity at 607 nm. Each experiment was repeated on three separate occasions.

2.15 | Statistical analysis

Statistical analysis was carried out using SPSS for Windows version 24.0. Data distribution of most variables was significantly different from normal distributions; thus, non-parametric statistical procedures were used for all analyses presented here. Independent groups were compared using Kruskal-Wallis and Mann-Whitney *U* tests. Comparisons among groups are illustrated using box-and-whisker plots where the horizontal line inside the box represents the median and the box indicates the interquartile range (IQR; the middle 50%

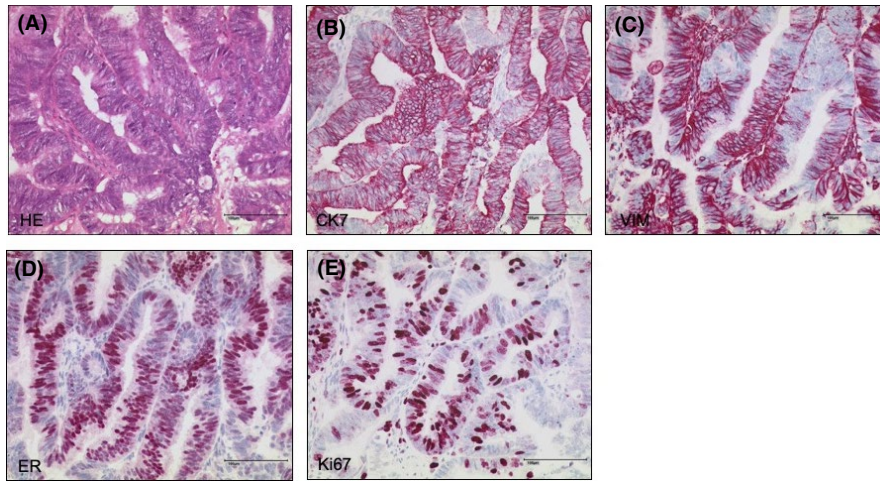


FIGURE 1 Histology and immunohistochemistry of ovarian cancer: A, H&E stain showing a confluent glandular growth pattern suggesting endometrioid carcinoma. B, CK7 expression as seen in adenocarcinomas of the gynecological tract. C, Scattered vimentin (VIM) expression in carcinoma cells, typical of endometrioid carcinoma. D, Most of the carcinoma cells show a nuclear positivity for estrogen receptor (ER). E, High proliferation rate of carcinoma cells as seen by Ki67 positivity. Altogether, these findings are diagnostic of an endometrioid adenocarcinoma. Original magnification, $\times 400$; scale bar, 100 μm

of scores). The ends of the whiskers denote the lowest and highest values still within 1.5 IQR of the lower and upper quartiles (ie, the lower and upper ends of the box), respectively. If there are no values >1.5 IQR below the lower or above the upper quartile (ie, outliers), the ends of the whiskers denote minimum and maximum of the data. All statistical tests were two-tailed and P values below .05 were considered to be statistically significant.

3 | RESULTS

3.1 | Patients and histopathological characteristics

In total, 60 patients with ovarian cancer and 20 healthy control biopsies were collected over a period of 6 years with a follow-up period

of 5-10 years after collection of the last sample. Patient age ranged from 21 to 82 years with a mean age of 60 years for the cancer group and from 38 to 71 years with a mean age of 56 years for the healthy controls. Of the affected patients, 52% died of cancer, 12% died of other reasons, and 36% of all ovarian cancer patients are still alive.

H&E staining together with the use of different ovarian cancer markers showed the histopathological diagnosis of ovarian cancer subtypes in the cancer patients (eg, endometrioid) as shown in Figure 1.

Most ovarian cancer patients presented with serous papillary ovarian cancer (71%), followed by mixed type tumors (14%) and endometrioid tumors (15%). Of all ovarian cancer patients, 85% had advanced tumor disease (T3). There were 76% of ovarian cancer patients with poorly differentiated tumors (G3), 19% presented with moderate tumor differentiation (G2), and 5% of the patients had

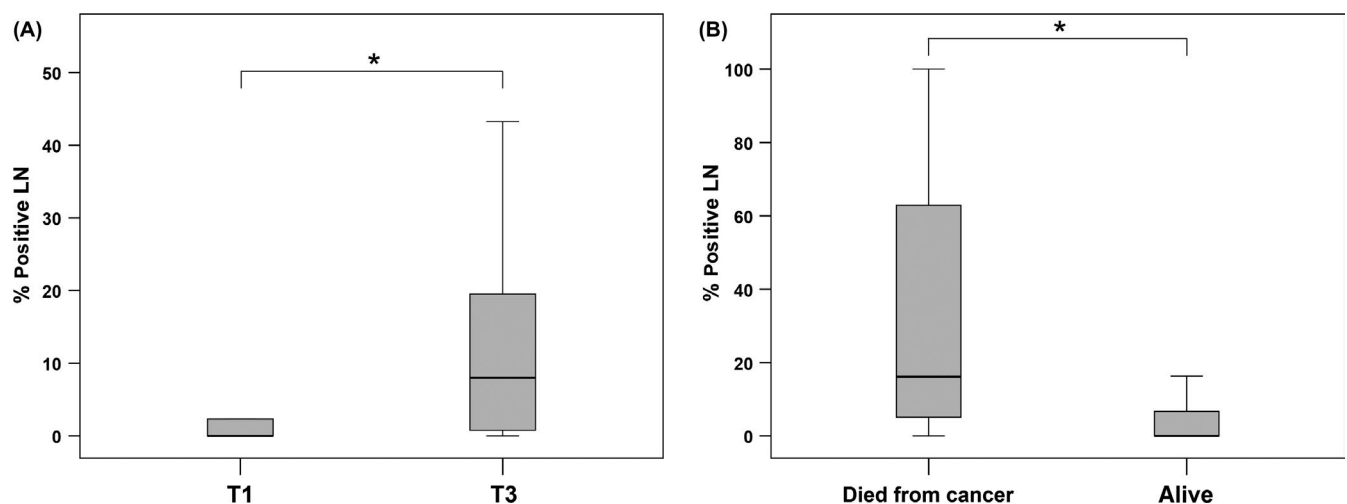


FIGURE 2 Comparison of the percentage of positive lymph nodes to total number of dissected lymph nodes in nodal-positive patients with respect to tumor stage (T1/T3) (A) or survival (B). Asterisk indicates significant differences

well-differentiated tumors (G1). Concerning the postoperative remaining tumor, 54% of our analyzed patients were operated without residual tumor remaining (TR 0), 28% had residual tumor ≤ 1 cm (TR 1), and 18% of the patients were left with a residual tumor >1 cm (TR 2). Of all patients, 72% fulfilled the criteria for lymphadenectomy. Of these patients 29% were nodal negative and 71% were nodal positive. Patients with advanced tumor stage (T3) had a significantly higher percentage of positive lymph nodes than patients with early tumor stage (T1) ($P = .037$; Figure 2A). Patients who died from ovarian cancer had a significantly higher percentage of positive lymph nodes than patients who are still alive ($P = .009$; Figure 2B). Table 1 summarizes the histopathological characteristics of the enrolled patients.

3.2 | Nectin-2 protein localization and quantification in ovarian cancer and peritoneal biopsies

In nearly all of our tumor biopsies, Nectin-2 protein was localized in the plasma membrane of cancer cells (Figure 3) which was identified by tumor cell markers as described earlier. Staining was particularly evident in regions in which the tumor still mimicked a glandular appearance, whereas other regions with tumor cell bulk

TABLE 1 Baseline patient and tumor characteristics of all 60 ovarian cancer patients randomized in the present study

Age (y)	
Median	60
Range	21-82
Tumor size	
pT1	7 (12%)
pT2	2 (3%)
pT3	51 (85%)
Lymph node metastasis (%) (72% of the operated patients)	
pN0	17 (28%)
pN+	43 (72%)
Histological grading (%)	
G1	3 (5%)
G2	11 (18%)
G3	46 (77%)
Histological type (%)	
Serous papillary	43 (72%)
Endometrioid	9 (15%)
Mixed type	8 (13%)
Tumor rest (TR) after surgery (%)	
TR 0	32 (54%)
TR 1	17 (28%)
TR 2	11 (18%)
Vital status (%)	
Alive	22 (36%)
Dead (from cancer)	31 (52%)
Dead (other reason)	7 (12%)

lacked any Nectin-2 staining (Figure 3F). CD31/Nectin-2 dual staining was found only for a few capillaries, indicating that the main source of protein synthesis of Nectin-2 are the tumor cells themselves (Figure 3G).

In the peritoneal biopsies, Nectin-2 was clearly localized in the endothelium of the peritoneal vasculature (Figure 4). In controls, staining appeared as a continuous inner circle of the vessel (Figure 4F,G). In peritoneal vasculature of tumor patients, this continuous circle is disrupted and dual staining was only evident in a few parts of the vessel. Quantitative analysis confirmed a significant decrease in these vessels in comparison to control (ie, $62.1\% \pm 6.1\%$ vs $91.1\% \pm 2.0\%$ [$P = .05$]).

3.3 | Nectin-2 gene expression in ovarian cancer biopsies

Comparison of Nectin-2 gene expression in tumor biopsies of our ovarian cancer patients with control (ovarian surface epithelium) showed higher expression levels in the tumor biopsies (Figure 5A). There were no significant detectable differences between histological subtypes (Figure 5B), grading, receptor status or distant metastasis.

However, we found significantly higher gene expression of Nectin-2 in tumor biopsies of patients with lymph node metastasis as compared to nodal negative patients ($P = .018$; Figure 5C).

In ovarian cancer biopsies of women in which the tumor was successfully removed during surgery (TR 0), Nectin-2 expression was lower as compared to women with an incomplete resection of the tumor (TR 1 or TR 2). This difference was significant ($P = .018$) for patients with >1 cm residual tumor after surgery (TR 2) in comparison to patients with no residual tumor (Figure 5D).

3.4 | Nectin-2 gene expression in peritoneal endothelium and VEGF serum levels in cancer patients in comparison to controls

In the peritoneal endothelium, Nectin-2 expression was significantly decreased ($P = .013$) in tumor patients compared to controls (Figure 6A). At the same time, VEGF was significantly increased ($P = .01$) clearly shown in the serum samples of tumor patients as compared to the serum levels of controls (Figure 6B).

No significant differences of Nectin-2 expression in peritoneal endothelium or serum VEGF levels were detectable regarding different histological subtypes, grading, nodal status or distant metastasis (not shown).

3.5 | Nectin-2 gene expression in endothelial cells, after VEGF stimulation, and VEGF inhibition with Flt-1/Fc in HUVEC culture

To further elucidate the degree to which VEGF affects Nectin-2 expression in endothelial cells, HUVEC were stimulated with VEGF, and Nectin-2 gene expression was measured. After treatment, Nectin-2

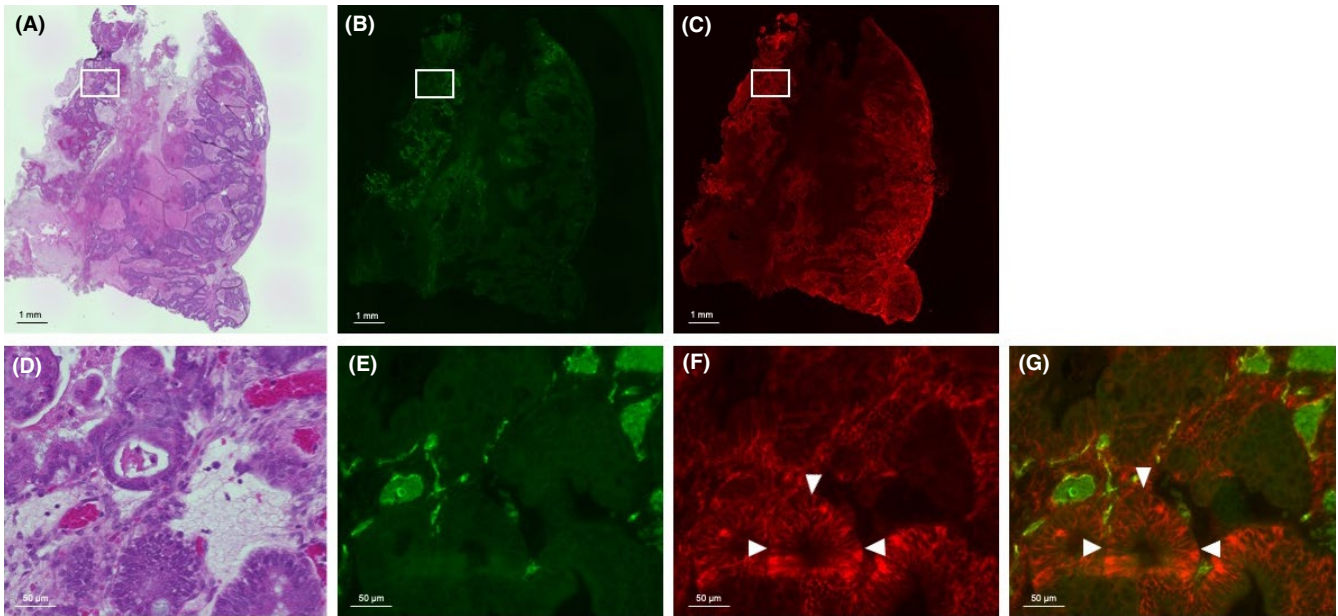


FIGURE 3 H&E staining of representative sections of ovarian cancer tissue (A). Immunocytochemical staining of CD 31 (green staining) or Nectin-2 (red staining) (B,C); scale bar, 1 mm. Detailed images D-G illustrate either H&E staining, immunocytochemical staining with CD31 (green staining), Nectin-2 (red-staining) or colocalization (yellow staining); scale bar, 50 μm . Note that in tumor biopsies most staining is found in tumor cells (arrowheads) (F) with only a few endothelial cells being positive for Nectin-2 (G). Pictures were taken with a fluorescence microscope under 40 \times magnification

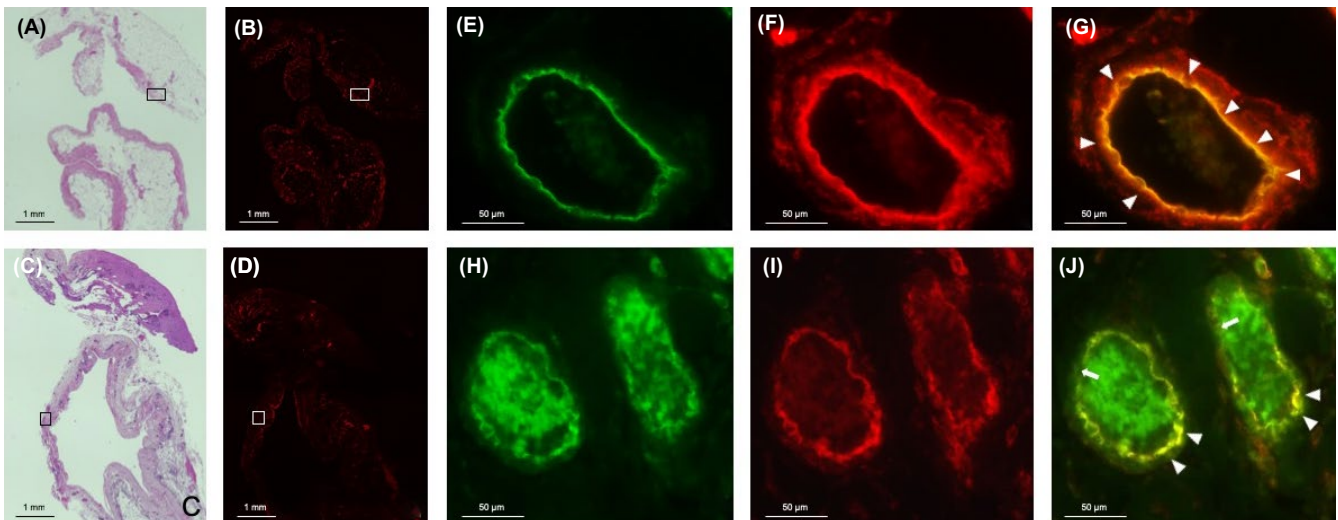


FIGURE 4 H&E staining of representative sections of peritoneal tissue of ovarian cancer patients (C) or immunocytochemical staining with Nectin-2 (D) in comparison to control peritoneal tissue (A,B); scale bar, 1 mm. Detailed representative immunocytochemical staining of Nectin-2 (red staining) (I) and colocalization (yellow staining) (J) with CD31 (green staining) (H) in endothelial cells (arrowheads) was carried out in comparison to control (E-G). In control peritoneal tissue samples, clear colocalization of CD31 and Nectin-2 can be seen (arrowheads) (G). Comparison of control tissue (G) with peritoneum of cancer patients (J) shows a decrease in endothelial cells positive for Nectin-2; scale bar, 50 μm . Pictures were taken with a fluorescence microscope under 40 \times magnification

expression was significantly downregulated ($P < .001$). This effect was significantly reversed by simultaneous inhibition of VEGF by Flt-1/Fc ($P < .001$). Interestingly, Nectin-2 expression after VEGF inhibition was significantly even higher ($P < .001$) as compared to Nectin-2 gene expression in control endothelium (HUVEC; Figure 7A).

3.6 | Effect of knockdown of Nectin-2 in HUVEC on endothelial permeability

To investigate the effect of Nectin-2 on permeability regulation, we carried out knockdown experiments by quantifying the relative

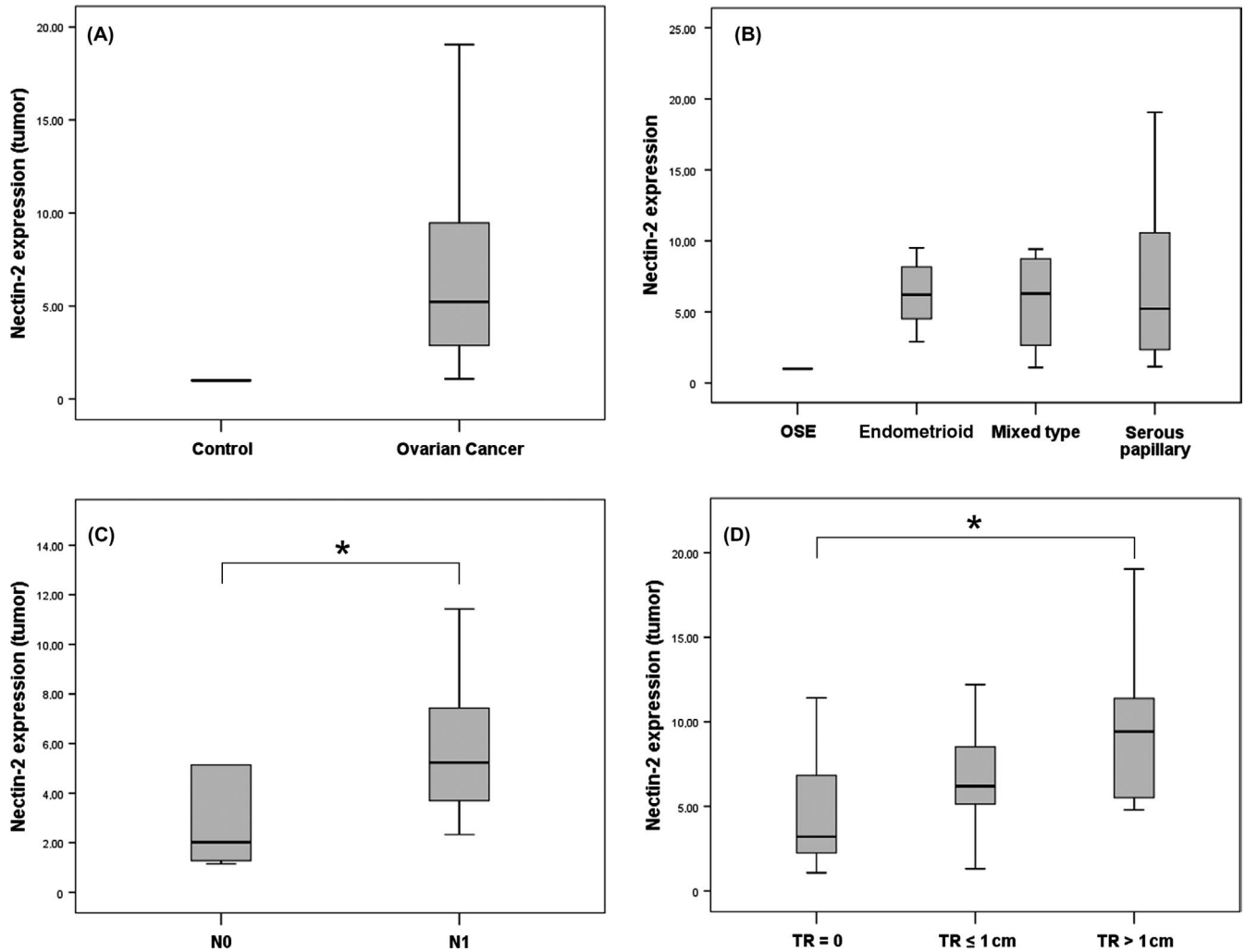


FIGURE 5 Comparison of relative Nectin-2 gene expression in the tumor (A) between ovarian cancer biopsies and ovarian surface epithelium (OSE), between different ovarian histological subtypes (B), between nodal-positive and -negative patients (C) and between resection status after surgery (D) (TR, residual tumor in cm). Asterisk indicates significant differences

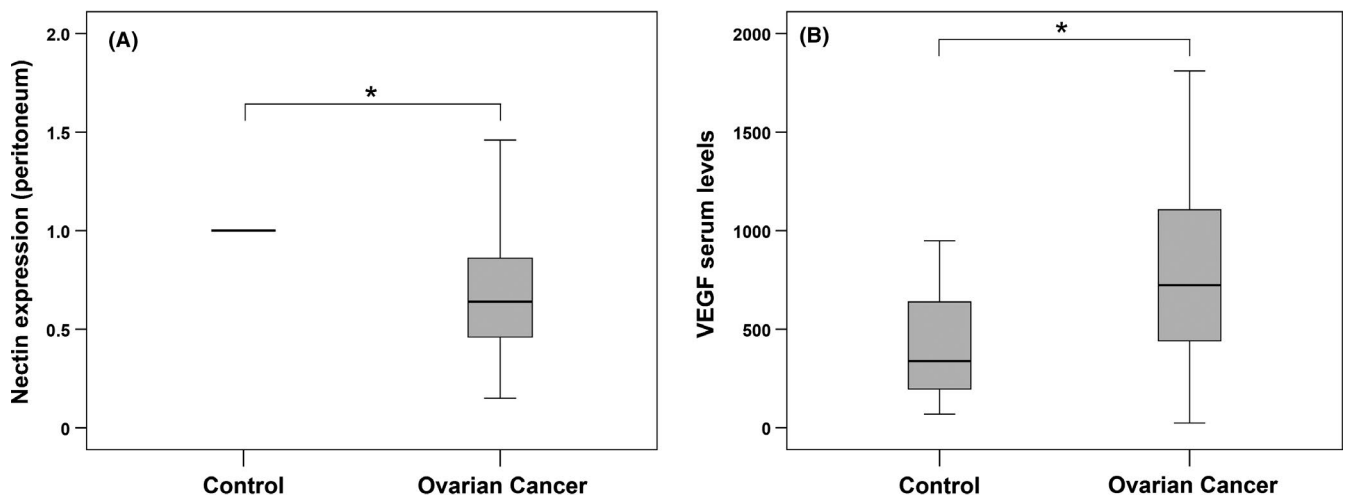


FIGURE 6 Comparison of relative Nectin-2 expression in the peritoneum of tumor patients and controls (A). Comparison of vascular endothelial growth factor (VEGF) serum levels in tumor patients in comparison to controls (B). Asterisk indicates significant differences

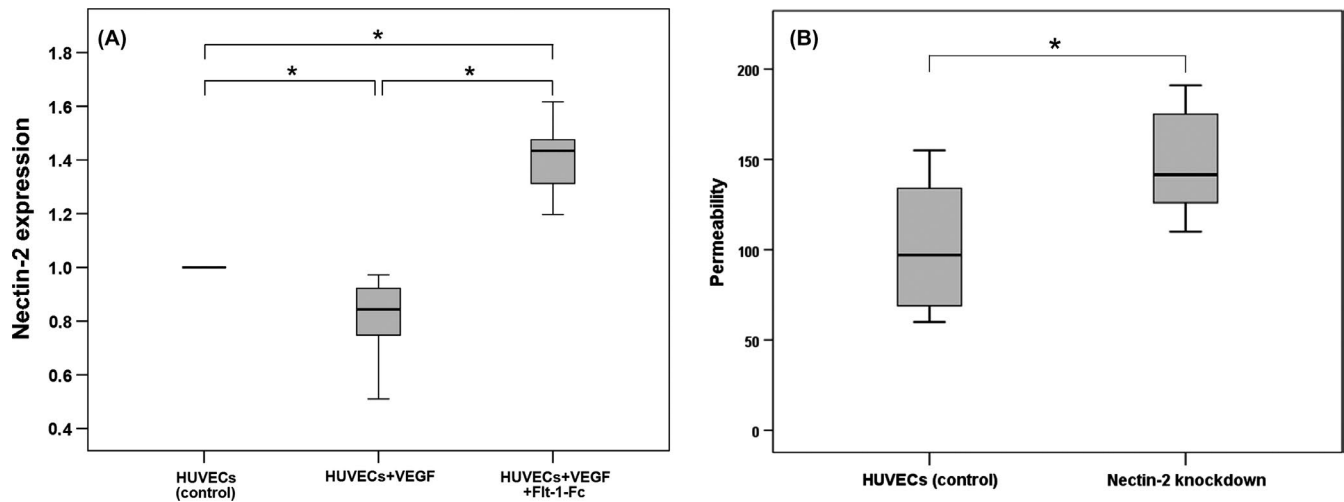


FIGURE 7 A, Comparison of relative Nectin-2 expression in HUVEC (as control) (first bar), after vascular endothelial growth factor (VEGF) stimulation (second bar) and simultaneous VEGF stimulation and inhibition with Flt-1/Fc (third bar). Note that VEGF inhibition with Flt-1/Fc led to a significant increase in Nectin-2 expression as compared to VEGF stimulation alone and to controls. B, Permeability of HUVEC (control) after knockdown of Nectin-2 for 72 h. The first bar represents the permeability of the control and the second bar of the cells after knockdown showing a significant increase in permeability. Asterisk indicates significant differences

permeability after knockdown of Nectin-2, showing a significant increase (Figure 7B; $P = .016$).

4 | DISCUSSION

Ovarian cancer is mostly diagnosed in an advanced stage of tumor.¹ At this stage, tumor cells have already spread into the abdominal cavity presenting as peritoneal tumor spread and metastasis. The cause of death is mostly associated with the mass of advanced abdominal tumor spread and abdominal tumor manifestation.^{27,28}

In the present study, we localized Nectin-2 in the tumor cells of ovarian cancer biopsies and found that Nectin-2 is highly expressed in ovarian cancer patients especially in nodal-positive patients and in those with >1 cm residual tumor after surgery (TR 2), namely patients who are known to be associated with a poor outcome.²⁷ A possible interpretation of this observation might be that tumor cell spread and dissemination into the abdominal cavity may be supported by increased peritoneal permeability as a result of downregulation of capillary adhesion proteins such as Nectin-2 in the peritoneal vasculature as shown in this study.

Recent studies have indicated that for local tumor spread into the abdominal cavity and to the peritoneal tissue, tumor cell migration and adhesion are the main mechanisms involved.²⁹ Although very few studies are available, molecules such as Nectins are described to be involved in these processes.^{8,17} These functions of Nectins implicate its possible roles in tumor cell survival and proliferation. In our study, we localized Nectin-2 protein mostly in the tumor cells in our human ovarian cancer biopsies and found higher gene expression of Nectin-2 in tumor cells of ovarian cancer patients in comparison to controls (ovarian surface epithelium). This observation is in line with investigations by Oshima et al.²⁰ By using expression profile

analysis, the authors showed overexpression of Nectin-2 in ovarian cancer tissue as compared to healthy controls. Moreover, recent studies have shown that Nectin-2 is highly expressed in epithelial malignancies and it was suspected that the expression correlates with high malignancy, fast progression, and/or poor prognosis of human breast cancer¹⁹ or gallbladder cancer.²¹ It was also demonstrated that inhibition of Nectin-2—using monoclonal antibodies—suppressed tumor cell proliferation in vitro.²⁰ The hypothesis that Nectin-2 supports tumor growth and metastasis by its function as an adhesion molecule is supported by our finding of significantly increased Nectin-2 expression in tumor biopsies of nodal-positive patients. In our collective patients in which lymphadenectomy had been carried out, 71% were affected with histologically proven lymph node metastasis, and patients who have already died from cancer had a significantly higher percentage of lymph node metastasis at the initial diagnosis as compared to patients who are still alive. In addition, in patients with advanced local stage tumors (T3), the percentage of positive lymph nodes was significantly higher than in early-stage ovarian cancer patients (T1). These results may lead to the suggestion that Nectin-2 is associated with more aggressive tumors characterized by lymph node metastasis. This finding is in line with results obtained by Liang et al.³⁰ concerning the significance of Nectin-2 in pancreatic ductal adenocarcinomas. They showed that Nectin-2 expression significantly correlated with clinical progression, as indicated by large tumor size and lymph node metastasis. Moreover, this study group found that positive Nectin-2 expression correlated with shorter survival. Investigations on other tumor entities such as multiple myeloma³¹ support these findings of Nectin-2 expression being closely related to the prognosis of disease.

The hypothesis that Nectin-2 supports tumor growth and metastasis is further supported by our findings that resection status after surgery is related to Nectin-2 expression. It is well known that

complete surgical removal of ovarian cancer is the main prognostic and survival factor for this tumor entity.^{27,32,33} In our study, patients in whom complete removal of the tumor was achieved showed significantly lower Nectin-2 expression in tumor biopsies as compared to patients in which a tumor residual of more than 1 cm remained. These results suggest that high tumor Nectin-2 expression in ovarian cancer may account for aggressive tumors and those associated with poor prognosis.

A second aspect of Nectin-2 functioning as a promotor of tumor cell spread may be seen in its potential involvement in ascites production. Ascites formation in ovarian cancer is known to facilitate the dissemination of cancer cells into the abdominal cavity.³⁴ In our previous investigations, we showed that increased peritoneal vascular permeability is due to VEGF-induced suppression of adhesion molecules in the peritoneal vasculature.²⁴ Furthermore, we showed that VEGF-derived ascites formation increases with aggressive ovarian cancer subtypes.²⁹ In the current study, we found Nectin-2 localized in the peritoneal vasculature. This is in line with the results of our previous studies where colocalization of the adhesion proteins claudin 5 and VE-cadherin, as well as decreased expression in the peritoneum of ovarian cancer patients, was found.^{24,29} In the current experiment, Nectin-2 was clearly suppressed in the peritoneal endothelium of tumor patients as compared to controls, associated with highly expressed VEGF in the tumor and increased VEGF serum levels indicating that Nectin-2 downregulation might be VEGF driven.

In our cell culture experiments, VEGF stimulation of endothelial cells resulted in significant downregulation of Nectin-2 that was not only reversed by simultaneous VEGF inhibition, but was also followed by significantly increased Nectin-2 expression as compared to controls. This interesting observation may be explained by additional suppression of endogenous VEGF synthesized by the endothelial cells themselves. Moreover, our finding that Nectin-2 knockdown in endothelial cells significantly increased endothelial permeability further supports the hypothesis that Nectin-2 plays a role in the regulation of permeability in the peritoneum. Taking these results together, it can be assumed that downregulation of Nectin-2 by VEGF, together with other adhesion proteins, supports the increase in vascular permeability to allow ascites production for local tumor dissemination. So far, it is not clear whether this is a direct effect of VEGF or whether the effect is indirectly achieved by downregulation of other adhesion proteins. In earlier studies, we showed that adhesion proteins influence each other. Knockdown of claudin 5 or VE-cadherin resulted in suppression of one or the other, respectively, and of Nectin-2 *in vitro*.³⁵ Both effects were associated with increased endothelial permeability. In the present study, we found that knockdown of Nectin-2 in HUVEC was followed by an increase in permeability, indicating that Nectin-2 is either directly or indirectly regulated by VEGF and, in this way, involved in permeability regulation that may facilitate local tumor spread into the abdominal cavity.

In summary, herein we showed that high expression of Nectin-2 in tumor cells of ovarian cancer patients is associated with early lymph node metastasis and residual tumor after surgery (TR 2),

resulting in a poor outcome for the patient. Downregulation of Nectin-2 in the peritoneal vasculature through the function of VEGF may increase vascular permeability followed by ascites production that further facilitates tumor dissemination in the abdominal cavity.

ACKNOWLEDGMENTS

This study was supported by the "Deutsche Forschungsgemeinschaft" (DFG) Bonn, Germany (DFG WU 319/3-2). We thank Tanja Köhler, Christa Ruckgaber and Regina Sauter for their excellent technical assistance in our laboratory.

CONFLICTS OF INTEREST

Authors declare no conflicts of interest for this article.

ORCID

Christine Wulff  <https://orcid.org/0000-0001-5827-5275>

REFERENCES

- Gerestein CG, Eijkemans MJ, Bakker J, et al. Nomogram for suboptimal cytoreduction at primary surgery for advanced stage ovarian cancer. *Anticancer Res.* 2011;31(11):4043-4049.
- Feigenberg T, Clarke B, Virtanen C, et al. Molecular profiling and clinical outcome of high-grade serous ovarian cancer presenting with low- versus high-volume ascites. *Biomed Res Int.* 2014;2014:1-9.
- Rosenberg SM. Palliation of malignant ascites. *Gastroenterol Clin North Am.* 2006;35(1):189-199.
- Hirabayashi K, Graham J. Genesis of ascites in ovarian cancer. *Am J Obstet Gynecol.* 1970;106(4):492-497.
- Ramakrishnan S, Subramanian IV, Yokoyama Y, Geller M. Angiogenesis in normal and neoplastic ovaries. *Angiogenesis.* 2005;8(2):169-182.
- Ooshio T, Kobayashi R, Ikeda W, et al. Involvement of the interaction of afadin with ZO-1 in the formation of tight junctions in Madin-Darby canine kidney cells. *J Biol Chem.* 2010;285(7):5003-5012.
- Miyoshi J, Takai Y. Molecular perspective on tight-junction assembly and epithelial polarity. *Adv Drug Deliv Rev.* 2005;57(6):815-855.
- Takai Y, Nakanishi H. Nectin and afadin: novel organizers of intercellular junctions. *J Cell Sci.* 2003;116(Pt 1):17-27.
- Morrison ME, Racaniello VR. Molecular cloning and expression of a murine homolog of the human poliovirus receptor gene. *J Virol.* 1992;66(5):2807-2813.
- Aoki N, Ujita M, Kuroda H, et al. Immunologically cross-reactive 57 kDa and 53 kDa glycoprotein antigens of bovine milk fat globule membrane: isoforms with different N-linked sugar chains and differential glycosylation at early stages of lactation. *Biochim Biophys Acta.* 1994;1200(2):227-234.
- Eberle F, Dubreuil P, Mattei MG, Devilard E, Lopez M. The human PRR2 gene, related to the human poliovirus receptor gene (PVR), is the true homolog of the murine MPH gene. *Gene.* 1995;159(2):267-272.
- Cocchi F, Lopez M, Menotti L, Aoubala M, Dubreuil P, Campadelli-Fiume G. The V domain of herpesvirus Ig-like receptor (HIgR) contains a major functional region in herpes simplex virus-1 entry into cells and interacts physically with the viral glycoprotein D. *Proc Natl Acad Sci USA.* 1998;95(26):15700-15705.

13. Satoh-Horikawa K, Nakanishi H, Takahashi K, et al. Nectin-3, a new member of immunoglobulin-like cell adhesion molecules that shows homophilic and heterophilic cell-cell adhesion activities. *J Biol Chem*. 2000;275(14):10291-10299.
14. Reymond N, Fabre S, Lecocq E, Adelaide J, Dubreuil P, Lopez M. Nectin4/PRR4, a new afadin-associated member of the nectin family that trans-interacts with nectin1/PRR1 through V domain interaction. *J Biol Chem*. 2001;276(46):43205-43215.
15. Mandai K, Nakanishi H, Satoh A, et al. Afadin: a novel actin filament-binding protein with one PDZ domain localized at cadherin-based cell-to-cell adherens junction. *J Cell Biol*. 1997;139(2):517-528.
16. Mandai K, Nakanishi H, Satoh A, et al. Ponsin/SH3P12: an I-afadin and vinculin-binding protein localized at cell-cell and cell-matrix adherens junctions. *J Cell Biol*. 1999;144(5):1001-1017.
17. Takahashi K, Nakanishi H, Miyahara M, et al. Nectin/PRR: an immunoglobulin-like cell adhesion molecule recruited to cadherin-based adherens junctions through interaction with Afadin, a PDZ domain-containing protein. *J Cell Biol*. 1999;145(3):539-549.
18. Takai Y, Irie K, Shimizu K, Sakisaka T, Ikeda W. Nectins and nectin-like molecules: roles in cell adhesion, migration, and polarization. *Cancer Sci*. 2003;94(8):655-667.
19. Martin TA, Lane J, Harrison GM, Jiang WG. The expression of the Nectin complex in human breast cancer and the role of Nectin-3 in the control of tight junctions during metastasis. *PLoS ONE*. 2013;8(12):e82696.
20. Oshima T, Sato S, Kato J, et al. Nectin-2 is a potential target for antibody therapy of breast and ovarian cancers. *Mol Cancer*. 2013;12:60.
21. Miao X, Yang ZL, Xiong L, et al. Nectin-2 and DDX3 are biomarkers for metastasis and poor prognosis of squamous cell/adenosquamous carcinomas and adenocarcinoma of gallbladder. *Int J Clin Exp Pathol*. 2013;6(2):179-190.
22. Karabulut M, Gunaldi M, Alis H, et al. Serum nectin-2 levels are diagnostic and prognostic in patients with colorectal carcinoma. *Clin Transl Oncol*. 2016;18(2):160-171.
23. Bates DO, Harper SJ. Regulation of vascular permeability by vascular endothelial growth factors. *Vascul Pharmacol*. 2002;39(4-5):225-237.
24. Herr D, Sallmann A, Bekes I, et al. VEGF induces ascites in ovarian cancer patients via increasing peritoneal permeability by downregulation of Claudin 5. *Gynecol Oncol*. 2012;127(1):210-216.
25. Lu Z, Chen J. Introduction of WHO classification of tumours of female reproductive organs, fourth edition. *Chinese J Pathol*. 2014;43(10):649-650.
26. Livak KJ, Schmittgen TD. Analysis of relative gene expression data using real-time quantitative PCR and the 2^{-Delta Delta C(T)} Method. *Methods*. 2001;25(4):402-408.
27. Bristow RE, Tomacruz RS, Armstrong DK, Trimble EL, Montz FJ. Survival effect of maximal cytoreductive surgery for advanced ovarian carcinoma during the platinum era: a meta-analysis. *J Clin Oncol*. 2002;20(5):1248-1259.
28. Chi DS, Eisenhauer EL, Zivanovic O, et al. Improved progression-free and overall survival in advanced ovarian cancer as a result of a change in surgical paradigm. *Gynecol Oncol*. 2009;114(1):26-31.
29. Bekes I, Friedl TWP, Köhler T, et al. Does VEGF facilitate local tumor growth and spread into the abdominal cavity by suppressing endothelial cell adhesion, thus increasing vascular peritoneal permeability followed by ascites production in ovarian cancer? *Mol Cancer*. 2016;15(1):13.
30. Liang S, Yang Z, Li D, et al. The clinical and pathological significance of Nectin-2 and DDX3 expression in pancreatic ductal adenocarcinomas. *Dis Markers*. 2015;2015:379568.
31. El-Sherbiny YM, Meade JL, Holmes TD, et al. The requirement for DNAM-1, NKG2D, and NKp46 in the natural killer cell-mediated killing of myeloma cells. *Cancer Res*. 2007;67(18):8444-8449.
32. Cascales Campos P, Gil J, Parrilla P. Morbidity and mortality outcomes of cytoreductive surgery and hyperthermic intraperitoneal chemotherapy in patients with primary and recurrent advanced ovarian cancer. *Eur J Surg Oncol*. 2014;40(8):970-975.
33. Eisenkop SM, Spirtos NM, Friedman RL, Lin W-CM, Pisani AL, Peticucci S. Relative influences of tumor volume before surgery and the cytoreductive outcome on survival for patients with advanced ovarian cancer: a prospective study. *Gynecol Oncol*. 2003;90(2):390-396.
34. Al Habyan S, Kalos C, Szyzborski J, McCaffrey L. Multicellular detachment generates metastatic spheroids during intra-abdominal dissemination in epithelial ovarian cancer. *Oncogene*. 2018;37(37):5127-5135.
35. Herr D, Fraser HM, Konrad R, Holzheu I, Kreienberg R, Wulff C. Human chorionic gonadotropin controls luteal vascular permeability via vascular endothelial growth factor by down-regulation of a cascade of adhesion proteins. *Fertil Steril*. 2013;99(6):1749-1758.

How to cite this article: Bekes I, Löb S, Holzheu I, et al. Nectin-2 in ovarian cancer: How is it expressed and what might be its functional role? *Cancer Sci*. 2019;110:1872-1882. <https://doi.org/10.1111/cas.13992>